

PLASMA CONVECTION IN THE HIGH-LATITUDE IONOSPHERE DEDUCED FROM CLUSTER EDI DATA AND THE IMF B_x COMPONENT

M. Forster¹, Y.I. Feldstein², L.I. Gromova², L.A. Dremukhina², A.E. Levitin², S.E. Haaland^{3,4}

¹ GFZ German Research Centre for Geosciences, Helmholtz Centre Potsdam, 14473 Potsdam, Germany

² IZMIRAN, Russian Academy of Science, Troitsk, Moscow region, Russia

³ Max Planck Institute for Solar System Research, 37191 Katlenburg-Lindau, Germany

⁴ Department of Physics and Technology, University of Bergen, Norway

Abstract. The relatively large data set of the Cluster Electron Drift Instrument (EDI) allows to perform statistical studies about the influence of the B_x -component of the Interplanetary Magnetic Field (IMF) on the high-latitude plasma convection pattern. The data set was divided into two approximately equal parts with $B_x > 0$ (IMF toward the sun) and $B_x < 0$ (IMF away from the sun) at the magnetopause. Then each part was sorted with respect to IMF orientation in the GSM y - z -plane into 8 sectors of 45° width. The derivation of high-latitude convection parts, that might be controlled by the IMF B_x component, has been carried out with two different methods that make use of IMF sectors 2 and 6 only, i.e. IMF orientation with $B_z \approx 0$ and $B_y > 0$ and $B_y < 0$, respectively. The first is based on the assumption of the absence of any B_x influence for equal signs of the IMF B_x and B_y components. The second makes use of the fact, that an opposite orientation of the IMF and the tail lobe field favours the entry of solar wind plasma into the polar cap region. The cross-polar cap potential difference at both hemispheres of the main night side convection cells of all 8 sectors does not reveal any distinct influence of B_x . On the other hand, there are indications of some influence of the IMF B_x component on the high-latitude day side circulation cells in sector 0 (for northward IMF).

Introduction

The ionospheric plasma convection at high latitudes appears as the characteristic feature of the interaction between solar wind, magnetosphere and ionosphere [Axford and Hines, 1961]. The decisive parameters for the control of this convection turned out to be the orientation and intensity of the Interplanetary Magnetic Field (IMF) [Dungey, 1961]. Various empirical coupling functions were proposed that can represent best the interaction between the solar wind and the magnetosphere [Newell et al., 2007]. The vast majority of these functions make use of the IMF B_z and B_y components, and only Akasofu's ϵ parameter applies the intensity of the full magnetic field vector, including all three IMF components [Perreault and Akasofu, 1978].

There are different positions in the public literature on the role of the IMF B_x component on geophysical processes at high latitudes, ranging from noticeable effects [Crooker, 1986; Belenkaya, 1998; Bloomberg et al., 2005; Newell et al., 2009; Peng et al., 2010] to unverifiable influences of this component on the high-latitude geophysical processes by Levitin et al. [1982], Holzworth and Meng [1984], and Newell et al. [1989]. The challenge to deduce any influence of the IMF B_x component on geophysical phenomena is due to the predominant sector structure of the IMF in the ecliptic plane, which consists of two different sectors, in each of which the IMF B_x and B_y components have opposite signs. Analysing geomagnetic field variations at near-polar regions in dependence on IMF B_x and B_y , Friis-Christensen et al. [1972] as well as Sumaruk and Feldstein [1973] concluded, that they are controlled solely by the IMF B_y component. This conclusion was based on analyses of the relations between geomagnetic field variations and the IMF components during periods, where this sector structure was disturbed and both components pointed in one and the same direction. This result obtained by them is now generally accepted and all known statistic high-latitude convection models of the ionospheric plasma describing the spatial-temporal convection pattern rely on the IMF B_z and B_y components only [cf., e.g., Haaland et al., 2007]. Investigations, on the other hand, which describe the connection between the plasma convection and the IMF B_x component, are as a rule global MHD simulation studies [e.g., Chapman et al., 2004; Peng et al., 2010]. As far as we know, up to now there are no publications on direct observations, which provide an unchallengeable evidence for ionospheric convection contributions, that are controlled by the IMF B_x component.

Data

The European Space Agency (ESA) Cluster mission consists of four identical spacecraft flying in a tetrahedron-like formation. Cluster has a nearly 90° inclination elliptical orbit with perigee initially around $4 R_E$ and apogee around $19 R_E$, and an orbital period of about 57 h. More than 10 millions individual "good" plasma drift measurements of the Electron Drift Instrument (EDI) on board Cluster within the region of data collection inside the magnetosphere were obtained from February 2001 up to now. They are assembled in about 20000 h of 1-min averages and mapped along the magnetic field lines into the upper ionosphere (~ 400 km) by use of the Tsyganenko-2001 (T01)

geomagnetic field model. The methodology of determining the electric field potential pattern in dependence of the IMF orientation were described in detail by the companion papers of *Haaland et al.* [2007] and *Förster et al.* [2007].

The relatively large EDI data set allows to perform statistical studies about the influence of the IMF B_x component on the high-latitude plasma convection pattern. For this purpose, the data set was divided into two approximately equal parts with $B_x > 0$ (IMF toward the Sun) and $B_x < 0$ (IMF away from the sun) at the magnetopause. Then each part was sorted with respect to IMF orientation in the GSM y - z -plane into 8 sectors of 45° width. The average amplitude of the IMF B_x component varies between 2 nT and 4 nT, with ~ 2 nT in those regions, where B_x and B_y are co-aligned, and ~ 4 nT within the usual sector structures with opposite signs of these components.

The IMF B_x component and the high-latitude ionospheric convection

Table 1 lists the potential differences ΔU between the night side (main) convection foci for all 8 sectors of the Northern and Southern Hemispheres and the two subsets with $B_x > 0$ and $B_x < 0$. The data show that not only the characteristic pattern are kept for both subsets, but also the regularity of cross-polar potential changes with the IMF: ΔU increases monotonically from sector 0 ($B_z > 0$, northward IMF) via positive IMF B_y values to sector 4 ($B_z < 0$, southward IMF) and then decreases again for negative IMF B_y from sector 4 to 0. This regularity is kept at the Southern Hemisphere without exception, but on the Northern Hemisphere there is an exception for sector 5 and $B_x < 0$. We suppose that this exceptional case is due to an insufficient data coverage: firstly, because of the increasing Cluster orbit tilt toward South, so that there are more data at the Southern compared with the Northern Hemisphere and, secondly, due to the much smaller amount of data within sectors of co-aligned IMF B_x and B_y components. The survey of ΔU at both hemispheres for different IMF B_x orientations (Table 1) does not reveal any distinct influence of B_x on night time the cross-polar cap potentials.

Table 1. Cross-polar cap potential differences ΔU between the night side (main) convection foci (in kV) for all the 8 sectors of different IMF orientation deduced from Cluster EDI measurements within the years 2001-2009, sorted for both IMF toward the Sun ($B_x > 0$) and away from the Sun ($B_x < 0$).

Sector	IMF orientation	ΔU (kV)		ΔU (kV)	
		Northern Hemisphere		Southern Hemisphere	
		$B_x > 0$	$B_x < 0$	$B_x > 0$	$B_x < 0$
0	B_z^+	15.8	14.4	14.2	12.4
1	B_z^+ / B_y^+	21.8	24.6	22.9	23.4
2	B_y^+	35.4	34.0	37.9	37.9
3	B_z^- / B_y^+	50.8	44.5	47.2	48.2
4	B_z^-	58.5	54.6	52.5	57.4
5	B_z^- / B_y^-	44.2	59.4	49.5	49.7
6	B_y^-	32.9	35.9	33.4	34.8
7	B_z^+ / B_y^-	17.7	24.2	21.9	20.6

follows:

$$U_0 = ([\text{sector 2 for } B_x > 0] + [\text{sector 6 for } B_x < 0]) / 2 ;$$

$$\hat{U}_{+y} = ([\text{sector 2 for } B_x > 0] - [\text{sector 6 for } B_x < 0]) / 9.75 \text{ (for } \hat{U}_{-y} \text{ we have the opposite sign of convection).}$$

In the second step we calculate the possible IMF B_x -dependent part of the convection using:

$$\hat{U}_{+x} = ([\text{sector 6 for } B_x > 0] - [U_0 + \hat{U}_{-y} \times 5.36]) / 3.6$$

$$\hat{U}_{+x} = ([\text{sector 2 for } B_x < 0] - [U_0 + \hat{U}_{+y} \times 5.30]) / 3.9$$

The second method draws upon the circumstance, that the Earth's dipole magnetic field lines over the northern polar cap region have an opposite direction to the IMF field lines for $B_x < 0$, but over the southern for $B_x > 0$. An opposite direction of the IMF and the magnetospheric tail magnetic field constitutes a favourable condition for the penetration of solar wind plasma into the polar cap region [Newell et al., 2009]. An enhanced flow of soft energetic particles can likewise affect the convection due to an increased level of ionisation of the upper atmosphere. The possible IMF B_x dependence of convection over the Northern Hemisphere we also get in two steps:

We made further an attempt to find out parts of the high-latitude convection, which might be controlled by IMF B_x . As described below, this attempt considered two different methods which are based on different assumptions.

The first method draws upon the presumption that the IMF B_x component does not have an effect for the geomagnetic variations recorded at the Earth's surface and for the convection in case of equally directed B_x and B_y , i.e., at the Northern Hemisphere and $B_x > 0$ this is the case for sectors 1, 2, and 3, while for $B_x < 0$ this is valid for sectors 5, 6, and 7. In the further calculations we consider only sectors 2 and 6, where the influence of IMF B_z is practically vanishing and the convection pattern becomes therefore more simple.

The B_x dependent part of convection, if it ever exists, we are going to isolate in two steps. First we calculate the BCP elements, which are free of the B_x influence, as

$$U_0 = ([\text{sector 2 for } B_x > 0] + [\text{sector 6 for } B_x > 0]) / 2 ;$$

$$\hat{U}_{+y} = ([\text{sector 2 for } B_x > 0] - [\text{sector 6 for } B_x > 0]) / 9.9 \text{ (for } \hat{U}_{-y} \text{ we have the opposite sign of convection).}$$

$$\hat{U}_{-x} = ([\text{sector 6 for } B_x < 0] - [U_0 + \hat{U}_{-y} \times 5.2]) / 2.3.$$

For the corresponding relations for the IMF B_x dependence at the Southern Hemisphere we obtain with analogous formulas of the two methods described above (not shown here).

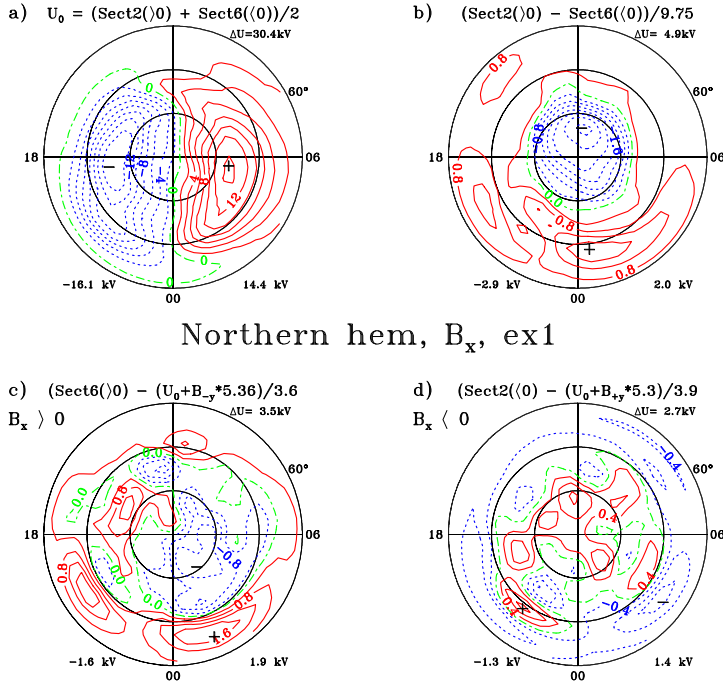


Figure 1. Basic Convection Pattern (BCP) derived from Cluster EDI observations of the Northern Hemisphere for various orientations of the IMF, using the first method of our B_x trial: a) basic convection part U_0 for vanishing IMF contribution, b) \hat{U}_{+y} part of the BCPs, describing the dependence on IMF B_y , normalized to 1 nT, c) and d) patterns resulting from the first method for IMF B_{+x} and B_{-x} dependence, respectively, normalized to 1 nT.

hand, evaluating the potential difference between the foci, which appear for northward IMF orientation, reveal some indications for an IMF B_x dependence. For an anti-parallel orientation of B_x and the geomagnetic force lines along

Table 2. Potential difference ΔU (in kV) for two BCPs (see text), based on Cluster EDI data for 2001-2009.

BCP element	Northern Hemisphere		Southern Hemisphere	
	Method 1	Method 2	Method 1	Method 2
U_0	30.4	29.5	33.3	30.9
\hat{U}_{+y}	-2.9	-3.0	2.8	2.5

the magnetospheric tail of the same hemisphere, the potential difference between the day side vortices appears to be slightly enhanced compared with the parallel orientation (Table 3). The potential difference is greater in that hemisphere where geomagnetic field lines and the IMF are oriented anti-parallel to each other.

Table 3. Potential differences ΔU between the high-latitude day side convection foci (in kV) of sector 0 deduced from Cluster EDI observations of 2001-2009, sorted both for IMF toward ($B_x > 0$) and away from the sun ($B_x < 0$).

Sector 0	Northern Hemisphere		Southern Hemisphere	
	$B_x > 0$	$B_x < 0$	$B_x > 0$	$B_x < 0$
	11.4	15.8	13.1	7.4

The significance of this effect and its statistical reliability has to proven yet in further studies.

Acknowledgments. This study is supported by the Deutsche Forschungsgemeinschaft (DFG), the RFBR grant 11-05-00306., and the Norwegian Research Council.

The characteristics of the potential pattern and the potential values of the BCP elements U_0 and $\hat{U}_{\pm y}$ (Figure.1 and Figure 2, Table 2) show a good agreement for both methods as well as with the previously determined values according to Förster *et al.* (2009, Figure. 2) with $U_0 = 31.0$ kV and $\hat{U}_{+y} = -3.2$ kV. Such a good correspondence can serve as an additional valid argument in favour of the legitimacy of the presumptions adopted for the calculation of the BCPs.

The characteristics and the intensity of the convection pattern deduced for $\hat{U}_{\pm x}$ is not that clear. There is no regular, systematic convection pattern, but rather some small randomly distributed vortices. The isolines are very irregular and the vortices have peak values, which are several times smaller than those related to the IMF B_y and B_z components. There didn't appear specific distributions, which could be related to the sign of IMF B_x or to hemispheric differences. We couldn't therefore reveal any conclusive evidences for the presence of the IMF B_x dependence in the convection pattern, its characteristics or intensity.

The analysis of the high-latitude daytime convection cells, on the other

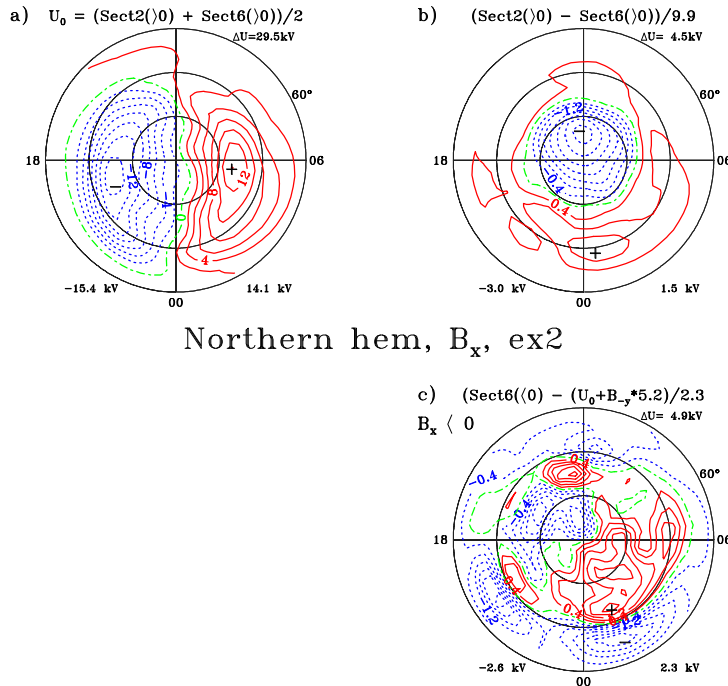


Figure 2: Basic Convection Pattern (BCP) derived from Cluster EDI observations of the Northern Hemisphere for various orientations of the IMF, using the second method of our B_x trial: a) basic convection part U_0 for vanishing IMF contribution, b) \hat{U}_{+y} part of the BCPs, describing the dependence on IMF B_y , normalized to $\ln T$, c) pattern resulting from the second method for IMF B_x dependence, normalized to $\ln T$.

Kletzing, High-latitude plasma convection from Cluster EDI: Variances and solar wind correlations, *Ann. Geophys.*, 25, 1691-1707, 2007.

Förster M., Y. I. Feldstein, S. E. Haaland, L. A. Dremukhina, L. I. Gromova, A. E. Levitin, Magnetospheric convection from Cluster EDI measurements compared with the ground-based ionospheric convection model IZMEM, *Ann. Geophys.*, 27, 3077-3087, 2009.

Friis-Christensen E., K. Lassen, J. Wilhjelm, J.M. Wilcox, W. Gonzalez, D.S. Colburn, Critical component of the Interplanetary Magnetic Field responsible for large geomagnetic effects in the polar cap, *J. Geophys. Res.*, 77, 3371-3376, 1972.

Haaland S.E., G. Paschmann, M. Förster, J. M. Quinn, R.B. Torbert, C.E. McIlwain, H. Vaith, P.A. Puhl-Quin, C.A. Kletzing, High-latitude plasma convection from Cluster EDI measurements: method and IMF-dependence, *Ann. Geophys.*, 25, 239-253, 2007.

Holzworth R.H., Meng C.-I., Auroral boundary variations and the interplanetary magnetic field, *Planet. Space Sci.* 32, 25-39, 1984.

Levitin A.E., R.G. Afonina, B.A. Belov, Y.I. Feldstein, Geomagnetic variations and field-aligned currents at northern high-latitudes and their relations to solar wind parameters, *Philos. Trans. Roy. Soc.*, A304, 253-301, 1982.

Newell P.T., C.-I. Meng, D.G. Sibeck, R. Lepping, Some low-altitude cusp dependencies on the Interplanetary Magnetic Field, *J. Geophys. Res.*, 94, 8921-8927, 1989.

Newell, P. T., T. Sotirelis, K. Liou, C. I. Meng, and F. J. Rich, A nearly universal solar wind magnetosphere coupling function inferred from 10 magnetospheric state variables, *J. Geophys. Res.*, 112, A01206, doi: 10.1029/2006JA012015, 2007.

Newell P.T., K.Liou, G.R.Wilson, Polar cap particle precipitation and aurora: review and commentary, *J. Atmosph. Solar-Terr. Phys.*, 71, 199-215, 2009.

Peng Z., C. Wang, and Y.Q. Hu, Role of IMF B_x in the solar wind-magnetosphere-ionosphere coupling, *J. Geophys. Res.*, 115, A08224, doi:10.1029/2010A015454, 2010.

Perreault W. K., and S.-I. Akasofu, A study of geomagnetic storms, *Geophys. J. R. Astron. Soc.*, 54, 547-573, 1978.

Sumaruk P.V. and Feldstein Y.I., Sector structure of the interplanetary magnetic field and magnetic disturbances in nearpole region, *Kosm. Issl.* 11, 155-160, 1973.

References

Axford W.I. and C.O.Hines, A unifying theory of high-latitude geophysical phenomena and geomagnetic storms, *Can. J. Phys.*, 39, 1433-1464, 1961.

Belenkaya E.S., High-latitude ionospheric convection patterns dependent on the variable IMF orientation, *J. Atmosph. Solar-Terr. Phys.*, 60, 1343-1354, 1998.

Blomberg L.G., J.A. Cummnok, I. I. Alexeev, E.S. Belenkaya, S.Yu. Bobrovnikov, and V.V. Kalegaev, Transpolar aurora: time evolution, associated convection patterns, and a possible cause, *Ann. Geophys.*, 23, 1917-1930, 2005.

Chapman J.F., I.H. Cairns, J.G. Lyon, C.R. Bowhuizen, MHD simulations of Earth's bow shock: Interplanetary magnetic field orientation effects on shape and position, *J. Geophys. Res.*, 109, doi: 10.1029/2003JA010235, 2004.

Crooker N.U., An evolution of antiparallel merging, *Geophys. Res. Lett.*, 13, 1063-1066, 1986.

Dungey J.W., Interplanetary magnetic field and the auroral zones, *Phys. Rev. Lett.*, 6, 47-48, 1961.

Förster M., G. Paschmann, S. E. Haaland, J. M. Quinn, R.B. Torbert, H. Vaith, C.A.